DOI: 10.1021/ma101772f

Macromolecules
COMMUNICATION TO THE EDITOR

Homo- and Hetero-Particle Clusters Formed by Janus Nanoparticles with Bicompartment Polymer Brushes

Bingbing Wang,[†] Bing Li,[†] Bin Dong,[†] Bin Zhao,[‡] and Christopher Y. Li*,[†]

[†]*Department of Materials Science and Engineering, Drexel University, Philadelphia, Pennsylvania 19104, United States , and* [‡]*Department of Chemistry, University of Tennessee, Knoxville, Tennessee 37996, United States*

Received August 3, 2010
Revised Manuscript Received October 1, 2010

The past decade witnessed tremendous progresses in nanoparticle synthesis; nanoparticles can now be readily obtained with great control of size, size distribution, and chemical makeup.[1−3] The next challenge in the field is to assemble nanoparticles into desired structures for targeted applications.[2,4−8] Most often nanoparticles are passivated with an organic coating made up of surfactants/polymer brushes; this organic coating is uniform and centrosymmetric.[3,9] While the centrosymmetric coating prevents nanoparticles from aggregation and mediates their assembly, the symmetry of the resultant nanoparticle ensembles is limited, largely driven by close packing of the particles. However, if the centrosymmetry is broken by using bicompartment polymer brushes, the polymer brush-coated nanoparticles then become anisotropic and much more versatile structures are feasible.[10,11] These nanoparticles coated with bicompartment brushes can be viewed as one type of Janus nanoparticles (JNPs), the concept that was discussed by De Gennes in his Nobel lecture in 1991.[12] The Janus feature often leads to surfactant-like structures, and as De Gennes pointed out, their assembly properties are intriguing: for membranes comprised of closely packed JNPs, there are interstices between the particles, which allows for mass transport between the two sides (known as "*breathable skin*").[12]

In addition to the breathable skin De Gennes mentioned, JNPs have potential applications in self-assembly, surface control, and optical as well as electronic devices and they have recently gained much interests from the communities of materials science, chemistry, physics and biology.[13] Janus particles that have been reported include organic JNPs (such as dendrimers,[14−16] block copolymer micelles,[17−22] and nanofibers[23,24]) and hybrid JNPs (such as micrometer-size beads,[25−32] dumbbell-, acorn-, or raspberry-like clusters[13,33−35] and particles with bicompartment surfactants[36−38] and/or polymer brushes.[39−48]). However, disregarding the large body of work on Janus particle synthesis, study on their assembly behavior, which is the key interest in this field, is limited. Computer simulation has been used to demonstrate that Janus particles (or, patchy particles) can assemble into complex structures, which mimic living organisms such as bacteria.[10,11,49,50] Hong et al. recently demonstrated that Janus particles with opposite electric charge on two hemispheres can assemble into well-defined clusters having up to 13 particles.[51] With increasing ionic strength of the solution, 1 μm diameter Janus particles with hydrophobic and charged hemispheres assembled into branched wormlike strings.[52] Even fewer experimental works on JNPs with diameters smaller than 20 nm have been reported.[38] One example is that Hatton group synthesized ~20 nm Janus magnetic nanoparticles (Fe_3O_4) with poly(acrylic acid) PAA/sodium polystyrenesulfonate and PAA/poly(*N*,*N*-dimethylaminoethyl methacrylate) brushes. pH- and temperature-responsive assembly behavior was observed.[47]

*Corresponding author. E-mail: chrisli@drexel.edu.

Scheme 1. Schematic Representation of Janus Nanoparticles (a) and Nanoparticles Symmetrically Grafted with One-Component (b) as Well as Binary Mixed (c) Polymer Brushes

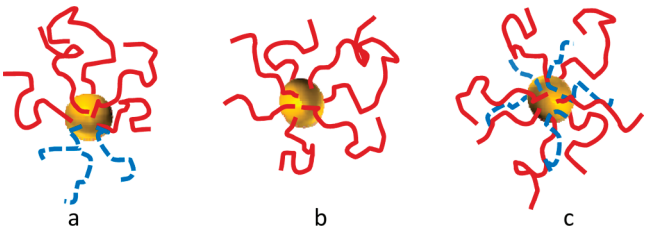

Herein we report homo- and heteroparticle clusters formed by Janus gold nanoparticles (J−AuNPs) with bicompartment polymer brushes composed of poly(methyl methacrylate) (PMMA) and poly(ethylene oxide) (PEO). Not only solution assembly behavior of these J−AuNPs has been systematically studied, heteroparticle clusters consisting of J−AuNPs and symmetrical magnetite nanoparticles (S−MNPs, Fe_3O_4) modified with PEO brushes have also been formed by controlled particle assembly in selected solvents. Furthermore, the assembly behavior of J−AuNPs was compared with that of the AuNPs symmetrically coated with PMMA/PEO mixed brushes. It is unambiguous that the unique assembly behavior of J−AuNPs was because of their Janus feature. These unique heteroparticle clusters are multifunctional particles, which may potentially find applications in bioimaging and drug delivery if semiconducting quantum dots and/or responsive polymer brushes are used to fabricate these clusters. Scheme 1 shows J−AuNPs and symmetric nanoparticles grafted with one-component polymer brushes as well as binary mixed polymer brushes.

Homoparticle assembly was investigated first. J−AuNPs with bicompartment PEO and PMMA brushes (PEO_{114}−Au_6−$PMMA_{208}$) were synthesized using the polymer-single-crystal-templating method as reported (Supporting Information).[41] The subscript numbers of PEO and PMMA denote the degrees of polymerization of the polymers while that of Au denotes the diameter of the nanoparticle in nanometers. The polydispersity indices (PDIs) of PEO and PMMA are 1.03 and 1.25, respectively. Gel permeation chromatography (GPC), thermogravimetric analysis (TGA) and ^{1}H NMR spectroscopy analysis showed that the overall grafting density of PEO and PMMA brushes was 0.52 chains/nm^2 (Supporting Information, Figures S1−S3). The average number of PEO and PMMA chains per AuNP is 32 and 26, respectively. The mass ratio of the PEO over PMMA is approximately 1: 3.2. These AuNPs grafted with bicompartment polymer brushes provide an ideal JNP system for self-assembly study. Solubility tests showed that they readily dissolved in good solvents of PEO and PMMA, such as acetone, chloroform, tetrahydrofuran, and dimethylformamide. To investigate the detailed solution assembly behavior, acetone and dioxane were chosen as model solvents. Upon dissolving PEO_{114}−Au_6−$PMMA_{208}$, the color of the acetone solution remained red over the entire observation period (one month), indicating that the particles were stable in acetone. However, the dioxane solution progressively changed from red to pale blue (Figure 1a). Figure 1b shows the UV/vis spectra of PEO_{114}−Au_6−$PMMA_{208}$

 Published on Web 10/26/2010

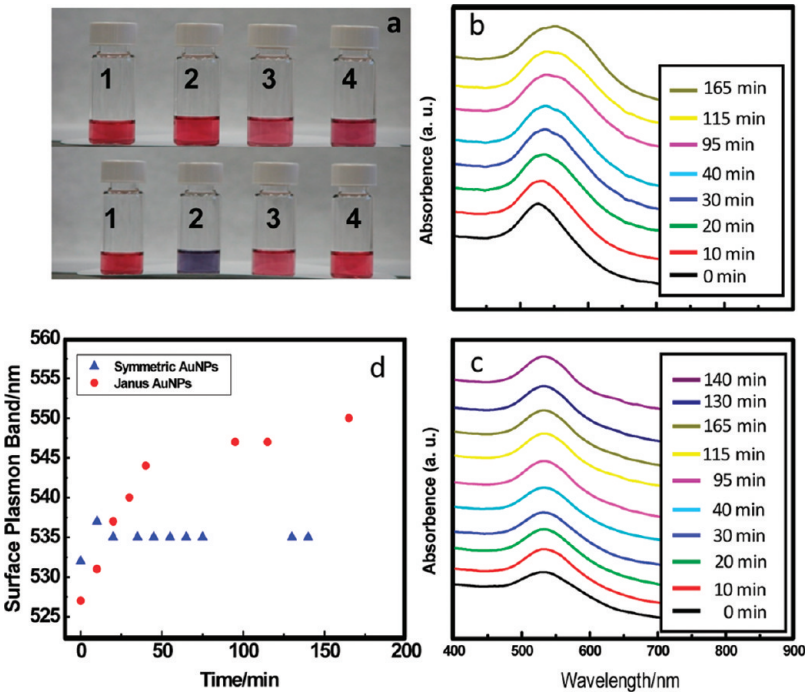

Figure 1. Solution assembly behavior of J−AuNPs and S−AuNPs. (a) Physical appearance of J−AuNPs (1, 2) and S−AuNPs (3, 4) in acetone (1, 3) and dioxane (2, 4) solutions after incubation for 1 min (top) and 90 min (bottom), UV/vis spectra of J−AuNPs (b) and S−AuNPs (c) in dioxane, and (d) SPR band position with respect to time for both J−AuNPs and S−AuNPs.

in dioxane. The surface plasmon resonance (SPR) absorption band red-shifted from 527 to 545 nm in ~50 min, and remained at 545−550 nm afterward. Both red shift of the SPR band and the color change of the solution suggest that nanoparticle assembly occurred, which caused delocalization of the surface plasmon of AuNPs.

TEM experiments were conducted to confirm particle assembly in dioxane. Samples were taken from the nanoparticle solution and spin coated on a carbon-coated Ni TEM grid to minimize particle aggregation during sample preparation. Figure 2 shows PEO_{114}−Au_6−$PMMA_{208}$ in dioxane at different times. JNPs were well dispersed in dioxane at the beginning. Small clusters of 2−7 JNPs can be seen for samples incubated for ~10 min (Figure 2b). The size of the cluster continuously increased and the ensemble became anisotropic, wormlike aggregates. After 35 min, the wormlike aggregates appeared to be branched, approximately 0.1−1 μm long and 50 nm wide (Figure 2d). There are approximately 7−15 nanoparticles along the short axis of the wormlike aggregates. This structure is remarkably similar to the recently reported ensemble formed by Janus particles with relatively large size, where compromise between hydrophobic interaction and charge repulsion at a given ionic strength led to the formation of wormlike particle strings.[52] In the present case, the wormlike aggregates are believed to be due to the bicompartment polymer brushes on these J−AuNPs. Dioxane is a relatively poor solvent for PEO.[53] Our previous experiments suggest that PMMA covers approximately 3/4 of the AuNP surface while PEO covers 1/4.[41] As previously mentioned, there are ~32 PEO and 26 PMMA chains per AuNP. This suggests that the local concentration of PEO is much higher than that of PMMA. Therefore, PEO "patches" prefer to be confined inside the aggregates so that the overall free energy of the system can be minimized. Note that the assembly is also reversible: as we add good solvent such as acetone into the system, the aggregates dissemble and the SPR band shifts back.

Note that nanoparticle chains can also be formed in symmetrically functionalized nanoparticles.[6,54−59] In order to demonstrate

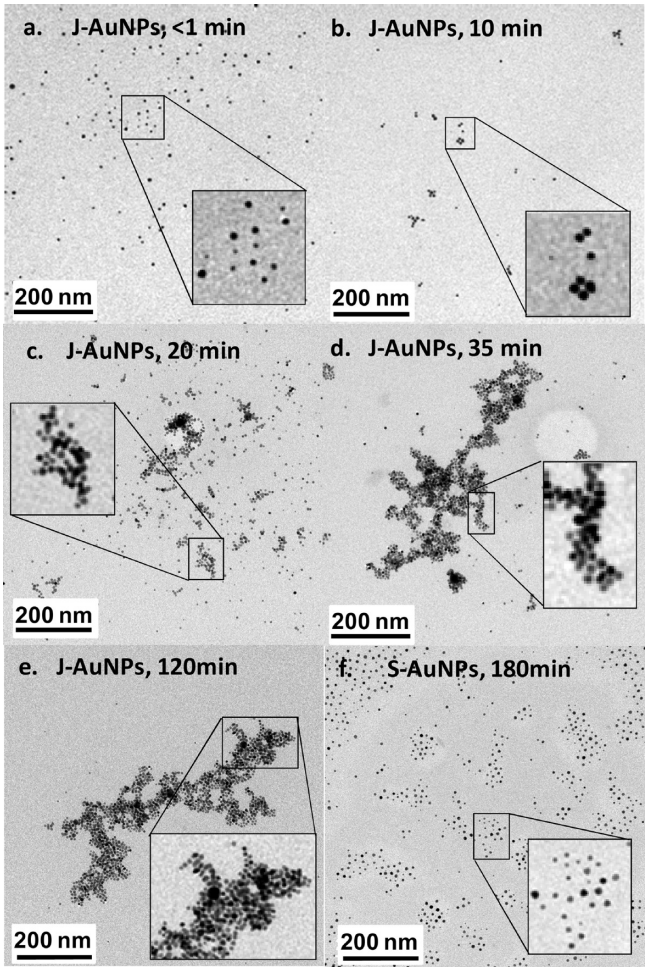

Figure 2. TEM micrographs of J−AuNPs (a−e) and S−AuNPs (f) in dioxane after various incubation times.

Scheme 2. Schematic Representations of the Assembly Behavior of J−AuNPs (a) and S−AuNPs (b) in Dioxane

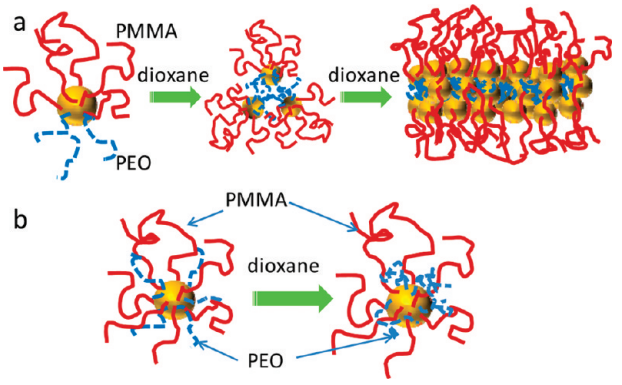

that the formation of the wormlike aggregates in the present case is because of the Janus feature of the nanoparticles, a control experiment was performed. We synthesized AuNPs symmetrically grafted with PEO/PMMA mixed brushes (S−AuNPs, $PEO_{114}/PMMA_{152}-Au_6$, Scheme 1c). Compared with J−AuNP $PEO_{114}-Au_6-PMMA_{208}$, S−AuNP $PEO_{114}/PMMA_{152}-Au_6$ has the same AuNP size. The molecular weights, PDIs of the polymer brushes, and the overall polymer grafting density are also comparable with those of the JNPs ($M_n^{PMMA} \sim 15.2$ K g/mol, $PDI^{PMMA} = 1.19$, $M_n^{PEO} \sim 5$K g/mol, $PDI^{PEO} = 1.03$, grafting density ~1.2 chains/nm^2). In the control experiment, these S−AuNPs were dissolved in acetone and dioxane and the assembly behavior was studied. The color as well as the SPR band position of the S−AuNP solution in acetone or dioxane did not change as compared to the J−AuNPs. Figure 1c shows the UV/vis spectra and Figure 1d shows the plot of the SPR band positions of J−AuNPs and S−AuNPs in dioxane against time. The SPR absorption band red-shifted for J−AuNPs while it remained constant for S−AuNPs. Figure 2f shows that after 3 h incubation in dioxane, S−AuNPs were well dispersed and aggregation was not observed. This clearly confirmed that the previous wormlike aggregate formation was due to the asymmetric property of JNPs. Scheme 2 shows the J−AuNP and S−AuNP assembly process in dioxane: for J−AuNPs, each particle has one PEO "patch". Since PEO tends to collapse in dioxane, the PEO patches of adjacent J−AuNPs tends to coalesce, leading to the formation of few particle clusters and wormlike aggregates (Scheme 2a). This is similar to the formation mechanism of wormlike micelles of block copolymers. However, for S−AuNPs, PEO and PMMA brushes are uniformly distributed on the nanoparticle surface. Although PEO chains also collapse in this case, because PMMA chains evenly spread on the entire particle surface and stabilize nanoparticles, the collapse of PEO chains does not lead to particle aggregation (Scheme 2b).

The above work suggests that collapsing of PEO chains in selective nonsolvents can lead to J−AuNP aggregation. Compared with the well studied pH/ionic strength mediated aggregation of symmetric nanoparticles, the present system is advantageous because the aggregation could be directional. In order to further explore this unique feature, we synthesized PEO-grafted symmetric MNPs (S−MNPs) to form AuNP−MNP heteroparticle clusters. The design is based on two reasons: (1) Tailored heteroparticle clusters of MNPs and AuNPs are multifunctional, having unique properties from both MNPs and AuNPs. (2) Symmetric PEO brushes were used for MNPs because, upon mixing with J−AuNPs with PEO and PMMA brushes, these PEO−MNPs can serve as "cross-linking points" where J−AuNPs can coalesce on. To this end, 5K g/mol PEO-grafted 15 nm MNPs ($PEO_{114}-MNP_{15}$) were synthesized as described in the Supporting Information. $PEO_{114}-MNP_{15}$ was incubated with J−AuNP $PEO_{114}-Au_6-PMMA_{208}$ and the weight ratio of these two types of nanoparticles ($r_{M/Au}$) was varied from 0 to 60:1. The mixture was first dissolved in acetone for 15 min with sonication. The same volume of dioxane was added dropwise and the mixture was stirred at room temperature for 24 h. Inset of Figure 3 shows the photo images of the solution color change with different $r_{M/Au}$. From left to right, $r_{M/Au}$ is ~5, 18, 44, and 60, respectively. The color of the solution changes from pale blue to pale red, which indicates that J−AuNPs are better dispersed with increasing $PEO_{114}-MNP_{15}$ concentration. UV−vis study supported this conclusion. Figure 3 shows that the SPR band of J−AuNPs blue-shifted from 557 to 529 nm when increasing $r_{M/Au}$ from 0 to 60:1. Note that MNPs used in this work did not show absorption at the wavelength around 400 to 700 nm.

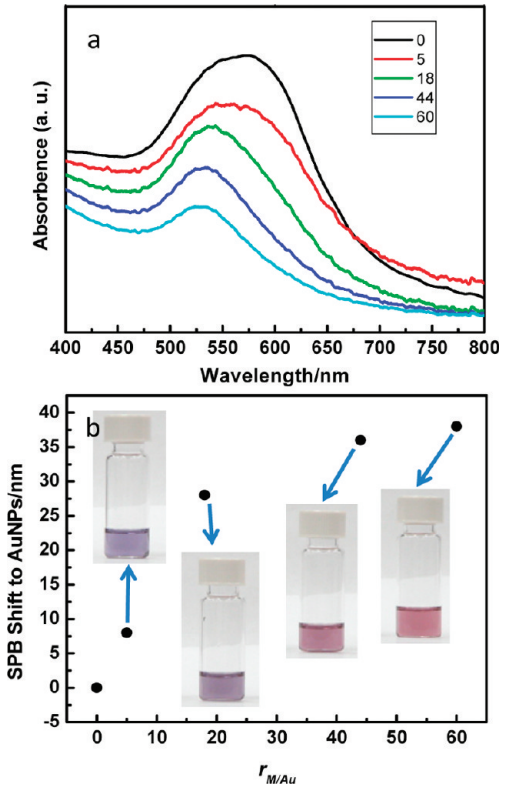

Figure 3. (a) UV/vis spectra of J−AuNP/S−MNP mixture at different S−MNP/J−AuNP ratios. (b) SPR band shift with respect to the S−MNP/J−AuNP ratio. Inset in part b shows the physical appearance of the corresponding solutions.

We further used TEM to study the assembly behavior of nanoparticles. As shown in Figure 4, compared with neat J−AuNPs, as S−MNPs were added at a 5:1 ratio, the wormlike aggregates were broken and heteroparticle clusters were formed, where the larger MNPs (lighter contrast) are in the center, surrounded by smaller AuNPs. The J−AuNP coating on the S−MNP is relatively uniform. As $r_{M/Au}$ increased from 5:1 to 60:1, J−AuNPs remained on the surface of S−MNPs while average particle number of AuNP per MNP (n_M/n_{Au}) decreased from 9 for $r_{M/Au} = 5$ to 6 for $r_{M/Au} = 18$, to 4 for $r_{M/Au} = 44$, and to 2 for $r_{M/Au} = 60$ (based on counting ~100−200 clusters, Supporting Information, Figure S4). This observation is consistent with the UV/vis results in Figure 3. When neat J−AuNPs were dissolved in dioxane/acetone (1:1, v/v) mixed solvent, wormlike aggregates formed. As PEO coated MNPs were added into the system, the uniform coating of PEO on the MNPs surface induced the PEO brushes on the J−AuNPs to collapse on MNPs, forming a "core-shell" type of heteroparticle ensemble stabilized by the outer PMMA brushes (insets in Figure 4b−e). As $r_{M/Au}$

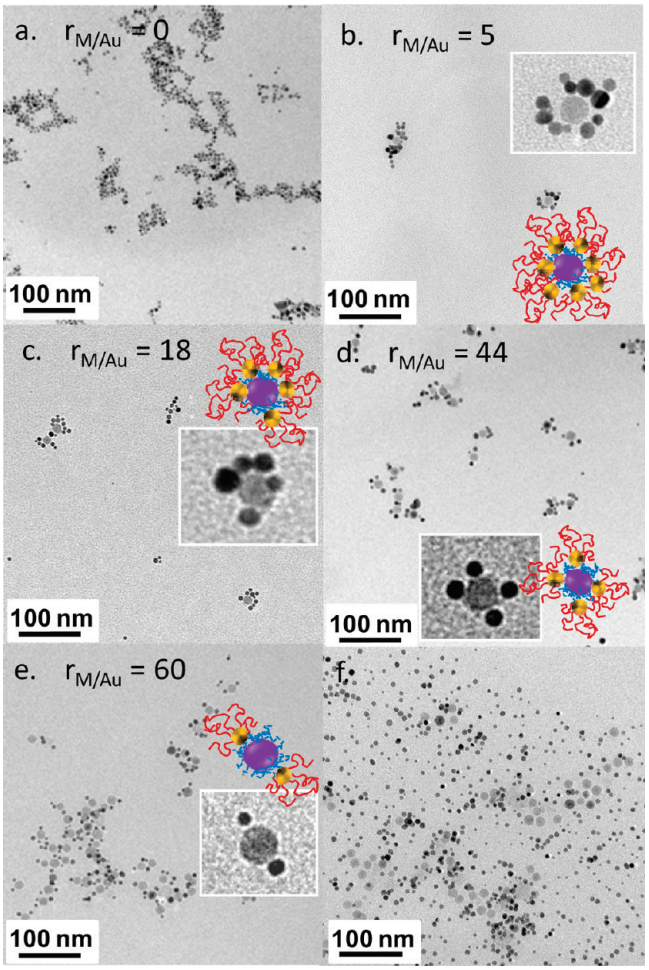

Figure 4. TEM micrographs of J−AuNP/S−MNP (PEO_{114}−Au_6−$PMMA_{208}$/PEO_{114}−MNP_{15}) ensembles at different S−MNP/J−AuNP ratios (a−e). Insets of parts b−e show enlarged images of heteroparticles clusters and the corresponding schematic illustrations. (f) TEM micrograph of S−AuNP (PEO_{114}/$PMMA_{152}$−Au_6) mixed with the same S−MNP (PEO_{114}−MNP_{15}). Because of uniformly distributed PEO and PMMA brushes on the nanoparticle surface, PEO mediated heteroparticle clusters were not observed.

Scheme 3. Schematic Representation of the Assembly Behavior of J−AuNPs and S−MNPs in Acetone/Dioxane (Top) and TEM Images of the Hetero-Clusters with Increasing S−MNP/J−AuNP Ratio (Bottom)

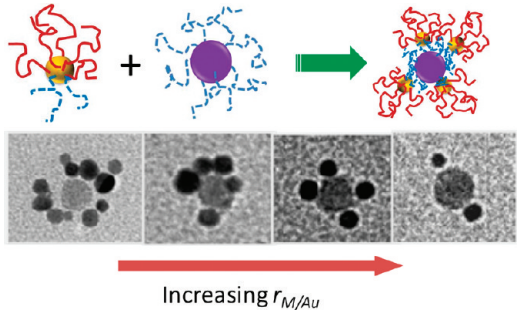

increases, the average AuNPs per MNPs decreased. Note that in the cases that S−MNPs were not completely covered with J−AuNPs, more anisotropic ensembles were formed as shown in Figure 4e. Scheme 3 shows the process of PEO induced heteroparticle cluster formation.

Control experiment was also performed with symmetric PEO_{114}/$PMMA_{152}$−Au_6 mixing with the same PEO_{114}−MNP_{15}. Because of the protection of PMMA brushes on the surface, the PEO chain on S−AuNPs was not able to collapse on the surface of S−MNPS. Uniformly dispersed AuNPs and MNPs mixture were observed as shown in Figure 4f. Note that the inset of Figure 4d resembles a CH_4 molecule with S−MNP and AuNPs representing C and H atoms, while the inset of Figure 4e mimics a H_2O molecule with S−MNP as the oxygen atom and AuNP as the H atom, respectively. Artificial molecules can thus be synthesized. The "bond angles" are not precisely controlled, nevertheless, these heteroparticle clusters have defined nanoparticle structures and particle ratio. More sophisticated techniques such as nanoparticle lithography may be needed to combine with the present technique to fabricate artificial molecules with precisely controlled bond angles.[60] It is also worthwhile to point out that this aggregation process is reversible and the clusters are responsive to solvent properties.

In conclusion, we have synthesized J−AuNPs with bicompartment polymer brushes consisting of PMMA and PEO. J−AuNPs were synthesized using the polymer-single-crystal-templating method and the grafting density of polymer brushes were characterized using TGA, GPC, and ^{1}H NMR. While the J−AuNP PEO_{114}−Au_6−$PMMA_{208}$ is soluble in good solvents for PMMA and PEO, interesting assembly behavior was observed in dioxane and dioxane/acetone mixed solvents. Few particle-clusters and wormlike aggregates were observed. Control experiment using symmetric AuNPs coated with PMMA and PEO mixed brushes confirmed that the assembly is because of the Janus feature of PEO_{114}−Au_6−$PMMA_{208}$. Intriguing heteroparticle clusters of PEO_{114}−Au_6−$PMMA_{208}$ and PEO_{114}−MNPs were obtained in dioxane/acetone mixed solvent and the formation mechanism was attributed to PEO-mediated particle assembly. The relative particle ratio can be controlled by varying the ratio of J−AuNPs and symmetric MNPs. These heteroparticle clusters are multifunctional and could potentially find applications in bioimaging as well as catalysis fields.

Acknowledgment. This work was supported by the NSF CBET-0730738.

Supporting Information Available: Text giving an experimental section and figures showing the ^{1}H NMR spectrum and TGA and GPC curves of PEO_{114}−Au_6−$PMMA_{208}$ and a histogram of the number of AuNPs per MNP. This material is available free of charge via the Internet at http://pubs.acs.org.

References and Notes

(1) Alivisatos, A. P. *Science* **1996**, *271*, 933–937.
(2) Murray, C. B.; Kagan, C. R.; Bawendi, M. G. *Annu. Rev. Mater. Sci.* **2000**, *30*, 545–610.
(3) Daniel, M. C.; Astruc, D. *Chem. Rev.* **2004**, *104*, 293–346.
(4) Bockstaller, M. R.; Mickiewicz, R. A.; Thomas, E. L. *Adv. Mater.* **2005**, *17*, 1331–1349.
(5) Balazs, A. C.; Emrick, T.; Russell, T. P. *Science* **2006**, *314*, 1107–1110.
(6) Srivastava, S.; Kotov, N. N. *Soft Matter* **2009**, *5*, 1146–1156.
(7) Claridge, S. A.; Castleman, A. W.; Khanna, S. N.; Murray, C. B.; Sen, A.; Weiss, P. S. *ACS Nano* **2009**, *3*, 244–255.
(8) Ofir, Y.; Samanta, B.; Rotello, V. M. *Chem. Soc. Rev.* **2008**, *37*, 1814–1825.
(9) Zhao, B.; Zhu, L. *Macromolecules* **2009**, *42*, 9369–9383.
(10) Glotzer, S. C. *Science* **2004**, *306*, 419–420.
(11) Glotzer, S. C.; Solomon, M. J. *Nat. Mater.* **2007**, *6*, 557–562.
(12) De Gennes, P. G. *Rev. Mod. Phys.* **1992**, *64*, 645–648.
(13) Perro, A.; Reculusa, S.; Ravaine, S.; Bourgeat-Lami, E. B.; Duguet, E. *J. Mater. Chem.* **2005**, *15*, 3745–3760.
(14) Ropponen, J.; Nummelin, S.; Rissanen, K. *Org. Lett.* **2004**, *6*, 2495–2497.
(15) Percec, V.; Imam, M. R.; Bera, T. K.; Balagurusamy, V. S. K.; Peterca, M.; Heiney, P. A. *Angew. Chem., Int. Ed.* **2005**, *44*, 4739–4745.

(16) Feng, X.; Taton, D.; Ibarboure, E.; Chaikof, E. L.; Gnanou, Y. *J. Am. Chem. Soc.* **2008**, *130*, 11662–11676.
(17) Erhardt, R.; Zhang, M. F.; Boker, A.; Zettl, H.; Abetz, C.; Frederik, P.; Krausch, G.; Abetz, V.; Muller, A. H. E. *J. Am. Chem. Soc.* **2003**, *125*, 3260–3267.
(18) Walther, A.; Muller, A. H. E. *Soft Matter* **2008**, *4*, 663–668.
(19) Wurm, F.; Kilbinger, A. F. M. *Angew. Chem., Int. Ed.* **2009**, *48*, 8412–8421.
(20) Ge, Z. S.; Xu, J.; Hu, J. M.; Zhang, Y. F.; Liu, S. Y. *Soft Matter* **2009**, *5*, 3932–3939.
(21) Voets, I. K.; Fokkink, R.; Hellweg, T.; King, S. M.; de Waard, P.; de Keizer, A.; Stuart, M. A. C. *Soft Matter* **2009**, *5*, 999–1005.
(22) Cheng, L.; Zhang, G. Z.; Zhu, L.; Chen, D. Y.; Jiang, M. *Angew. Chem., Int. Ed.* **2008**, *47*, 10171–10174.
(23) Srivastava, Y.; Marquez, M.; Thorsen, T. *Biomicrofluidics* **2009**, *3* (012801), 1–6.
(24) Bhaskar, S.; Lahann, J. *J. Am. Chem. Soc.* **2009**, *131*, 6650.
(25) Du, Y. Z.; Tomohiro, T.; Zhang, G.; Nakamura, K.; Kodaka, M. *Chem. Commun.* **2004**, 616–617.
(26) Cayre, O.; Paunov, V. N.; Velev, O. D. *J. Mater. Chem.* **2003**, *13*, 2445–2450.
(27) Cayre, O.; Paunov, V. N.; Velev, O. D. *Chem. Commun.* **2003**, 2296–2297.
(28) Love, J. C.; Gates, B. D.; Wolfe, D. B.; Paul, K. E.; Whitesides, G. M. *Nano Lett.* **2002**, *2*, 891–894.
(29) Correa-Duarte, M. A.; Salgueirino-Maceira, V.; Rodriguez-Gonzalez, B.; Liz-Marzan, L. M.; Kosiorek, A.; Kandulski, W.; Giersig, M. *Adv. Mater.* **2005**, *17*, 2014–2018.
(30) Hugonnot, E.; Carles, A.; Delville, M. H.; Panizza, P.; Delville, J. P. *Langmuir* **2003**, *19*, 226–229.
(31) Velev, O. D.; Lenhoff, A. M.; Kaler, E. W. *Science* **2000**, *287*, 2240–2243.
(32) Fujimoto, K.; Nakahama, K.; Shidara, M.; Kawaguchi, H. *Langmuir* **1999**, *15*, 4630–4635.
(33) Yin, Y. D.; Lu, Y.; Xia, Y. N. *J. Am. Chem. Soc.* **2001**, *123*, 771–772.
(34) Lu, Y.; Xiong, H.; Jiang, X. C.; Xia, Y. N.; Prentiss, M.; Whitesides, G. M. *J. Am. Chem. Soc.* **2003**, *125*, 12724–12725.
(35) Ohnuma, A.; Cho, E. C.; Camargo, P. H. C.; Au, L.; Ohtani, B.; Xia, Y. N. *J. Am. Chem. Soc.* **2009**, *131*, 1352–1353.
(36) Jackson, A. M.; Myerson, J. W.; Stellacci, F. *Nat. Mater.* **2004**, *3*, 330–336.
(37) Vilain, C.; Goettmann, F.; Moores, A.; Le Floch, P.; Sanchez, C. *J. Mater. Chem.* **2007**, *17*, 3509–3514.
(38) van Herrikhuyzen, J.; Portale, G.; Gielen, J. C.; Christianen, P. C. M.; Sommerdijk, N.; Meskers, S. C. J.; Schenning, A. *Chem. Commun.* **2008**, 697–699.
(39) Li, B.; Li, C. Y. *J. Am. Chem. Soc.* **2007**, *129*, 12–13.
(40) Li, B.; Ni, C.; Li, C. Y. *Macromolecules* **2008**, *41*, 149–155.
(41) Wang, B. B.; Li, B.; Zhao, B.; Li, C. Y. *J. Am. Chem. Soc.* **2008**, *130*, 11594–11595.
(42) Li, C. Y. *J. Poly. Sci. Poly. Phys.* **2009**, *47*, 2436–2440.
(43) Kim, B. J.; Bang, J.; Hawker, C. J.; Chiu, J. J.; Pine, D. J.; Jang, S. G.; Yang, S. M.; Kramer, E. J. *Langmuir* **2007**, *23*, 12693–12703.
(44) Liu, B.; Wei, W.; Qu, X. Z.; Yang, Z. H. *Angew. Chem., Int. Ed.* **2008**, *47*, 3973–3975.
(45) Berger, S.; Synytska, A.; Ionov, L.; Eichhorn, K. J.; Stamm, M. *Macromolecules* **2008**, *41*, 9669–9676.
(46) Zhang, J.; Jin, J.; Zhao, H. Y. *Langmuir* **2009**, *25*, 6431–6437.
(47) Lattuada, M.; Hatton, T. A. *J. Am. Chem. Soc.* **2007**, *129*, 12878–12889.
(48) Isojima, T.; Lattuada, M.; Vander Sande, J. B.; Hatton, T. A. *ACS Nano* **2008**, *2*, 1799–1806.
(49) Vanakaras, A. G. *Langmuir* **2006**, *22*, 88–93.
(50) Sciortino, F.; Giacometti, A.; Pastore, G. *Phys. Rev. Lett.* **2009**, *103*, 237801–4.
(51) Hong, L.; Cacciuto, A.; Luijten, E.; Granick, S. *Nano Lett.* **2006**, *6*, 2510–2514.
(52) Hong, L.; Cacciuto, A.; Luijten, E.; Granick, S. *Langmuir* **2008**, *24*, 621–625.
(53) Brandrup, J.; Immergut, E. H.; Grulke, E. A.; Abe, A.; Bloch, D. R., Ed. *Polymer Handbook*. John Wiley & Sons: New York, 2005.
(54) Lin, S.; Li, M.; Dujardin, E.; Girard, C.; Mann, S. *Adv. Mater.* **2005**, *17*, 2553–2559.
(55) Kang, Y. J.; Erickson, K. J.; Taton, T. A. *J. Am. Chem. Soc.* **2005**, *127*, 13800–13801.
(56) Benkoski, J. J.; Bowles, S. E.; Korth, B. D.; Jones, R. L.; Douglas, J. F.; Karim, A.; Pyun, J. *J. Am. Chem. Soc.* **2007**, *129*, 6291–6297.
(57) Fukao, M.; Sugawara, A.; Shimojima, A.; Fan, W.; Arunagirinathan, M. A.; Tsapatsis, M.; Okubo, T. *J. Am. Chem. Soc.* **2009**, *131*, 16344–16345.
(58) Mann, S. *Nat. Mater.* **2009**, *8*, 781–792.
(59) Nie, Z. H.; Fava, D.; Kumacheva, E.; Zou, S.; Walker, G. C.; Rubinstein, M. *Nat. Mater.* **2007**, *6*, 609–614.
(60) Snyder, C. E.; Ong, M.; Velegol, D. *Soft Matter* **2009**, *5*, 1263–1268.